New "D-State-Observer"-Based Vector Control for Sensorless Drive of Permanent-Magnet Synchronous Motors

Shinji Shinnaka, *Member, IEEE*

***Abstract*—This paper proposes a new sensorless vector control method that can be applied to both salient-pole and nonsalient-pole permanent-magnet synchronous motors (PMSMs). The proposed method estimates phase of rotor flux by a newly developed flux-state observer for sensorless vector control of PMSMs, which is referred to as the "D-state observer." The D-state observer has the following attractive features: 1) it requires no additional steady-state condition for the motor mathematical model; 2) its order is the minimum second; 3) a single observer gain is simply constant over a wide operating range, and easily designed; 4) it utilizes motor parameters in a very simple manner; and 5) its structure is very simple and can be realized at a very low computational load. Usefulness of the proposed method is examined and confirmed through extensive experiments.**

***Index Terms*—D-state observer, flux-state observer, minimum order, phase-locked loop (PLL), sensorless vector control, synchronous motor.**

I. Introduction

FOR the appropriate drive of a permanent-magnet synchronous motor (PMSM), information of rotor phase (in other words, position) is indispensable. However, mounting a rotational position sensor on a rotor causes several drawbacks from the viewpoints of reliability, cost, size, and cable wiring. In order to cope with the drawbacks, a number of sensorless vector control methods have been proposed so far. It has become a matter of common understanding that no single sensorless vector control method can operate appropriately in a wide speed range from zero to over rated speed, and that a frequency-hybrid combination of two methods is practical, either of which can operate appropriately in the zero-to-low-speed or low-to-high-speed range. From a practical viewpoint of the frequency-hybrid combination, it is still of value to develop a new sensorless vector control method that can operate appropriately in the low-to-high-speed range.

In sensorless control methods for a low-to-high-speed drive, the fundamental component of motor-driving voltage and current has been widely used for estimating rotor phase [1]–[7]. They can be classified into two categories in terms of estimating dynamics, one of which exploits electrical dynamics only [4]–[7], and the other exploits mechanical dynamics in addition to electrical dynamics [1]–[3]. Since mechanical dynamics are highly influenced by an uncertain load connected to PMSMs, the mechanical approach seems to lack general versatility or limits its applicability. The more general electrical approach could be classified according to the phase estimation principle into three categories, such as estimation of rotor flux by simple or modified integration, estimation of back electromotive force (EMF), or extended back EMF by a disturbance observer with steady-state condition, and estimation of rotor flux by state observer. The state observer directly estimating rotor flux has the following advantages over others: 1) it does not necessarily requires steady-state condition; 2) the convergence property of estimate can be analyzed more rigidly; and 3) consequently, it has potential to operate in the widest speed range.

An early contribution to flux-state-observer-based sensorless vector control for PMSMs would be the one by Yang *et al.* where the fourth full-order adaptive state observer in the stationary reference frame is constructed with steady-state condition for a nonsalient-pole PMSM [4]. Unfortunately, Yang's method lacks stability in variable-speed operation in addition to steady-state operation at near rated speed. Several modifications to Yang's method, such as improvement of stability by means of variable observer gains, extension to a salient-pole PMSM, extension to the rotational reference frame, etc., have been undertaken in [5]–[7].

This paper proposes a new sensorless vector control method based on new a flux-state observer that is completely different from both the fourth-order flux-state observer by Yang *et al.* [4]–[7] and the mechanical-state observer *et al.* [1]–[3]. The proposed state observer for sensorless vector control has the following attractive features.

1) It is a new flux-state observer requiring no additional steady-state condition for the dynamic mathematical model of the PMSM.
2) Its order is the minimum second.
3) Observer gain guaranteeing proper estimation in four quadrants over a wide operating range except singular zero speed is a simple constant, and can be easily designed.
4) It utilizes motor parameters in a very simple manner.
5) Its structure is very simple, and it can be realized at very low computational load.
6) It can be applied to both salient-pole and nonsalient-pole PMSMs.

Paper IPCSD-05-004, presented at the 2004 Industry Applications Society Annual Meeting, Seattle, WA, October 3–7, and approved for publication in the IEEE TRANSACTIONS ON INDUSTRY APPLICATIONS by the Industrial Drives Committee of the IEEE Industry Applications Society. Manuscript submitted for review July 11, 2004 and released for publication February 2, 2005.

The author is with the Department of Electrical Engineering, Kanagawa University, Yokohama 221-8686, Japan (e-mail: shinnaka@cc.kanagawa-u.ac.jp).

Digital Object Identifier 10.1109/TIA.2005.847282

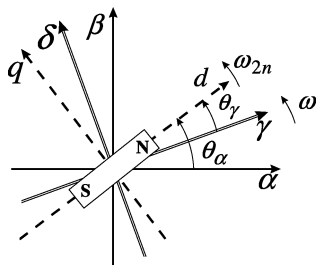

Fig. 1. Phase of rotor N-pole in γ–δ general reference frame rotating at arbitrary angular velocity ω.

This paper gives detailed designs and analyses for the state observer and the state-observer-based sensorless vector control system. Their validity and usefulness are examined and confirmed through extensive experiments.

Remark 1: In the following, the symbol "s" is used as a differential operator d/dt or as a Laplace operator with no comment as long as no confusion occurs.

II. D-State Observer

A. Mathematical Model

Consider the general reference frame where orthogonal γ–δ coordinates are rotating at an arbitrary instant angular velocity ω as shown in Fig. 1. Rotating polarity is defined such that the direction from principal axis (γ axis) to the secondary axis (δ axis) is positive. Note that all of the following 2×1 vector signals related to PMSMs are defined in the general reference frame.

The electromagnetic characteristics of PMSMs can be described as the following circuit equations:

$$\boldsymbol{v}_1 = R_1\boldsymbol{i}_1 + [s\boldsymbol{I} + w\boldsymbol{J}]\boldsymbol{\phi}_1 \tag{1}$$

$$\boldsymbol{\phi}_1 = \boldsymbol{\phi}_i + \boldsymbol{\phi}_m \tag{2}$$

$$\boldsymbol{\phi}_i = [L_i\boldsymbol{I} + L_m\boldsymbol{Q}(\theta_\gamma)]\,\boldsymbol{i}_1 \tag{3}$$

$$\boldsymbol{\phi}_m = \Phi\boldsymbol{u}(\theta_\gamma); \quad \Phi = \text{const} \tag{4}$$

$$\boldsymbol{Q}(\theta_\gamma) = \begin{bmatrix} \cos 2\theta_\gamma & \sin 2\theta_\gamma \\ \sin 2\theta_\gamma & -\cos 2\theta_\gamma \end{bmatrix} \tag{5}$$

$$\boldsymbol{u}(\theta_\gamma) = \begin{bmatrix} \cos\theta_\gamma \\ \sin\theta_\gamma \end{bmatrix} \tag{6}$$

$$s\theta_\gamma = \omega_{2n} - \omega \tag{7}$$

where 2×1 vectors $\boldsymbol{v}_1, \boldsymbol{i}_1$, and ϕ_1 are voltage, current, and flux of the stator, respectively, 2×1 vectors ϕ_i, ϕ_m are components of stator flux ϕ_1; more precisely, ϕ_i indicates flux evolved directly by stator current $\boldsymbol{i}_1$ and ϕ_m is flux due to rotor magnet, $\boldsymbol{I}$ is a 2×2 identity matrix, $\boldsymbol{J}$ is a 2×2 skew symmetric matrix such as

$$\boldsymbol{J} = \begin{bmatrix} 0 & -1 \\ 1 & 0 \end{bmatrix} \tag{8}$$

ω_{2n} is the electric speed of rotor, R_1 is stator resistance, L_i, L_m are the so-called "in-phase and mirror-phase inductances" having the following relation to the d, q-axes inductances [9]:

$$\begin{bmatrix} L_d \\ L_q \end{bmatrix} = \begin{bmatrix} 1 & 1 \\ 1 & -1 \end{bmatrix} \begin{bmatrix} L_i \\ L_m \end{bmatrix}. \tag{9}$$

B. State Equation and D-State Observer

From the circuit equation in (1)–(7), a new set of state equations in the general reference frame can be established as follows:

state equation:

$$s\boldsymbol{\phi}_m = [(\omega_{2n} - \omega)\boldsymbol{J}]\,\boldsymbol{\phi}_m \tag{10}$$

output equation:

$$[\boldsymbol{v}_1 - R_1\boldsymbol{i}_1 - [s\boldsymbol{I} + \omega\boldsymbol{J}]\boldsymbol{\phi}_i] = [\omega_{2n}\boldsymbol{J}]\boldsymbol{\phi}_m. \tag{11}$$

It is worth noting that the basic circuit equation in (1)–(3) is simply converted to the output equation in (11) and that the state equation in (10), which is a key equation, is established by simply differentiating (4) with respect to time. For the new set of state equations in (10) and (11), the following state-observer theorem can be newly established.

State-Observer Theorem:

1) Assume that the rotor flux ϕ_m is unknown, and that the other remaining signals are known. Under this assumption, consider the following state observer for estimating the rotor flux:

$$\left.\begin{aligned} \boldsymbol{D}(s,\omega)\tilde{\boldsymbol{\phi}}_1 &= \boldsymbol{G}[\boldsymbol{v}_1 - R_1\boldsymbol{i}_1] + \omega_{2n}[\boldsymbol{I} - \boldsymbol{G}]\boldsymbol{J}\hat{\boldsymbol{\phi}}_m \\ \hat{\boldsymbol{\phi}}_m &= \tilde{\boldsymbol{\phi}}_1 - \boldsymbol{G}\phi_i \end{aligned}\right\} \tag{12}$$

where $\boldsymbol{D}(s,\omega)$ is the so-called 2×2 "D-module" defined as [8]

$$\boldsymbol{D}(s,\omega) = s\boldsymbol{I} + \omega\boldsymbol{J} \tag{13}$$

and $\boldsymbol{G}$ is a single 2×2 observer gain such as

$$\boldsymbol{G} = g_1\boldsymbol{I} - \text{sgn}(\omega_{2n})g_2\boldsymbol{J}, \qquad g_1 = \text{const}; \quad g_2 = \text{const} > 0. \tag{14}$$

The estimate $\hat{\phi}_m$ of rotor flux by (12) converges to the actual one except for zero speed.

2) In the case where ω_{2n}, ω are constant, the convergence rate of the flux estimate to the actual one is given by $\exp(-|\omega_{2n}|g_2 t)$.

Proof:

1) Applying (13) and (14) to (12) and rearranging yields

$$s\hat{\boldsymbol{\phi}}_m = \boldsymbol{G}\Big[\boldsymbol{v}_1 - R_1\boldsymbol{i}_1 - [s\boldsymbol{I} + \omega\boldsymbol{J}]\phi_i - \omega_{2n}\boldsymbol{J}\hat{\boldsymbol{\phi}}_m\Big] + (\omega_{2n} - \omega)\boldsymbol{J}\hat{\boldsymbol{\phi}}_m. \tag{15}$$

Subtracting the state equation in (10) from (15) yields

$$s[\hat{\boldsymbol{\phi}}_m - \boldsymbol{\phi}_m] = \boldsymbol{G}\left[\boldsymbol{v}_1 - R_1\boldsymbol{i}_1 - [s\boldsymbol{I} + \omega\boldsymbol{J}]\boldsymbol{\phi}_i - \omega_{2n}\boldsymbol{J}\hat{\boldsymbol{\phi}}_m\right] + (\omega_{2n} - \omega)\boldsymbol{J}[\hat{\boldsymbol{\phi}}_m - \boldsymbol{\phi}_m]. \tag{16}$$

Applying the output equation in (11) to (16) establishes the following error equation:

$$s[\hat{\boldsymbol{\phi}}_m - \phi_m] = [-\omega_{2n}\boldsymbol{G} + (\omega_{2n} - \omega)\boldsymbol{I}]\,\boldsymbol{J}[\hat{\phi}_m - \phi_m]. \tag{17}$$

Using (14), (17) reduces to

$$s[\hat{\boldsymbol{\phi}}_m - \phi_m] = -\left[|\omega_{2n}|g_2\boldsymbol{I} + (\omega + (g_1 - 1)\omega_{2n})\,\boldsymbol{J}\right][\hat{\boldsymbol{\phi}}_m - \boldsymbol{\phi}_m]. \tag{18}$$

A 2×2 matrix of the error equation in (18) has a pair of complex conjugate eigenvalues λ_1, λ_2 such as

$$\begin{bmatrix}\lambda_1\\ \lambda_2\end{bmatrix} = \begin{bmatrix}-\left(|\omega_{2n}|g_2 + j\left(\omega + (g_1 - 1)\omega_{2n}\right)\right)\\ -\left(|\omega_{2n}|g_2 - j\left(\omega + (g_1 - 1)\omega_{2n}\right)\right)\end{bmatrix} \tag{19}$$

where j indicates imaginary part of complex number. Real part of the eigenvalues is negative under the condition of g_2 in (14) except for zero speed. Equations (18) and (19) with negative real part implies that the estimation error converges to zero except for zero speed, i.e., it constitutes the first part of the theorem.

2) Using the eigenvalues, (18) can be converted into the following equivalent error equation:

$$s\tilde{\boldsymbol{e}} = \mathrm{diag}(\lambda_1, \lambda_2)\tilde{\boldsymbol{e}} \tag{20}$$

with

$$\tilde{\boldsymbol{e}} = \frac{1}{\sqrt{2}}\begin{bmatrix}1 & j\\ 1 & -j\end{bmatrix}[\hat{\boldsymbol{\phi}}_m - \boldsymbol{\phi}_m]. \tag{21}$$

In the case where ω_{2n}, ω are constant, the solution of (20) is given as

$$\tilde{\boldsymbol{e}} = \mathrm{diag}(e^{\lambda_1 t}, e^{\lambda_2 t})\tilde{\boldsymbol{e}}_o \tag{22}$$

where $\tilde{\boldsymbol{e}}_o$ is an initial value of $\tilde{\boldsymbol{e}}$. Equations (21) and (22) yield the following relation:

$$\|\hat{\boldsymbol{\phi}}_m - \boldsymbol{\phi}_m\| = \|\tilde{\boldsymbol{e}}\| = \exp\left(-|\omega_{2n}|g_2 t\right)\|\tilde{\boldsymbol{e}}_o\|. \tag{23}$$

Equation (23) implies the second part of the theorem.

Note that the convergence of the flux estimate to the actual one except for zero speed requires no condition of constant ω_{2n}, ω as rigorously proved in the proof of part 1) of the theorem. The reason that part 2) of the theorem employs the constant conditions is simply for deriving analytically a single constant convergence rate.

The flux-state observer in (12) is referred to as the D-state observer in the following. It can be depicted as in Fig. 2. As clearly seen in Fig. 2, if the observer gain would be selected as a 2×2 identity matrix, i.e., $g_1 = 1, g_2 = 0$, the D-state observer reduces to the simple voltage model. Practical selections of the observer gain are, e.g., $g_1 = 1$, $g_2 > 0$, $g_1 = 0$, and $g_2 > 0$. Addition of the computational load of the D-state observer to the voltage model is a few multiplications by a single constant gain $g_2 > 0$, and is very small.

It is apparent that the D-state observer has the following attractive features.

1) It requires no additional steady-state condition for the motor mathematical model.
2) Its order is the minimum second.
3) A single 2×2 observer gain is simply constant over a wide operating range, and easily designed based on (19) and (23).
4) It utilizes motor parameters in a very simple manner.
5) Its structure is very simple, and it can be realized at very low computational load (refer to *Remark 3* below).

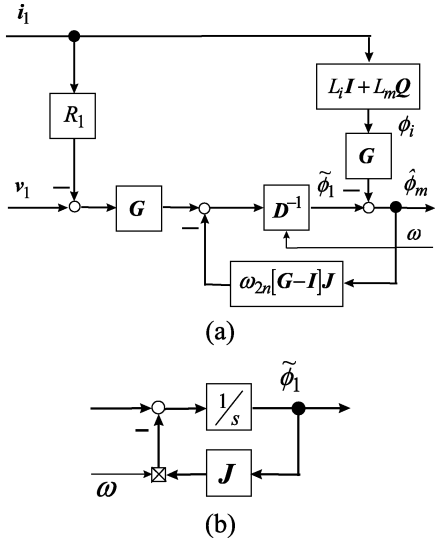

Fig. 2. D-state observer for estimating rotor flux. (a) Total configuration. (b) Realization of the $\boldsymbol{D}^{-1}(s, \omega)$.

6) It can deal with a salient-pole PMSM as well as a non-salient-pole one.

Remark 2: It is apparent from the circuit equation in (1)–(7) that the rotor flux exerts no influence upon stator voltage and current at steady standstill. This means the fact that no methods using driving stator voltage and current can continuously estimate rotor flux at steady standstill, and that zero speed is a singular point for the methods. The fact is applied to the proposed D-state observer without exception.

Remark 3: The state of the art in the fourth full-order flux-state observer for sensorless drives requires two 2×2 matrix observer gains equivalent to eight scalar gains. In addition, for the stable drive of a salient-pole PMSM, the gains cannot be constant, and should be varying dependent on motor speed [5]. This fact reinforces the simplicity and relative light computational load of the D-state observer as a flux-state observer.

III. Sensorless Vector Control

A. Generalized Integral-Type Phase-Locked loop (PLL)

One of the universal methods to make rotating coordinates to orient the rotor N-pole is the one constructing a PLL where the γ axis of the rotating orthogonal coordinates is locked to the phase of the rotor N-pole. One such PLL is the generalized integral-type PLL where rotor speed can be estimated simultaneously with locked phase with no additional computational load [9]. The generalized integral-type PLL can be summarized as in the following theorem [9].

Generalized Integral-Type PLL Theorem: Let $\hat{\theta}_\alpha$, $\hat{\omega}_{2n}$ be estimates of rotor N-pole phase θ_α in the stationary reference frame and electrical speed ω_{2n}, respectively. Construct the generalized integral-type PLL such as (refer to Fig. 3)

$$\left.\begin{aligned}\omega &= C_{\mathrm{PLL}}(s)\theta_\gamma\\ \hat{\omega}_{2n} &= \omega\\ \hat{\theta}_\alpha &= \tfrac{1}{s}\omega\end{aligned}\right\} \tag{24}$$

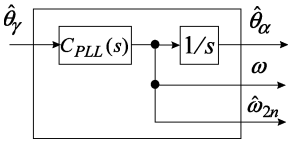

Fig. 3. Configuration of the generalized integral-type PLL.

where $C_{\rm PLL}(s)$ is the "Phase Controller" in the rational form of

$$C_{\rm PLL}(s) = \frac{C_n(s)}{C_d(s)} = \frac{c_{nm}s^m + c_{nm-1}s^{m-1} + \cdots + c_{n0}}{s^m + c_{dm-1}s^{m-1} + \cdots + c_{d0}}. \quad (25)$$

If the following two conditions are satisfied:

1) the phase controller is designed such that polynomial $H(s)$ in (26) is the Hurwitz

$$H(s) = sC_d(s) + C_n(s) \quad (26)$$

2) the asymptotic property in (27) holds

$$sC_d(s)\theta_\alpha \to 0 \quad (27)$$

then estimates $\hat{\theta}_\alpha$, $\hat{\omega}_{2n}$ converge to actual values θ_α, ω_{2n}, respectively (refer to [9] for proof).

If the estimate of rotor mechanical speed ω_{2m} is required, it is determined from the electrical one such as

$$\hat{\omega}_{2m} = \frac{\hat{\omega}_{2n}}{N_p} \quad (28)$$

where $\hat{\omega}_{2m}$, N_p are the estimate of rotor mechanical speed and number of pole pairs, respectively.

B. Sensorless Vector Control System

Fig. 4 shows a total configuration of the sensorless vector control system using the D-state observer. The difference from the standard sensor vector control system is the existence of the "Phase Estimator" block. The phase estimator produces two estimates of rotor phase evaluated on the α axis and rotor electrical speed from the two inputs of stator current and stator voltage command in the rotating reference frame. Of course, actual voltage can be used instead of its command at the cost of additional hardware. The rotor mechanical speed estimate is determined from its electrical one according to (28) and transferred to the speed controller.

Fig. 5 shows a configuration of the phase estimator consisting of two subblocks of the "D-State Observer" and the "Phase Synchronizer." The D-state observer produces rotor phase estimate $\hat{\theta}_\gamma$ evaluated on the γ axis of the rotating coordinates of speed ω by means of the current, voltage command on the same coordinates, coordinates speed ω, and rotor speed estimate $\hat{\omega}_{2n}$ (refer to Fig. 1).

Fig. 6 illustrates the structure of the D-state observer employed in Fig. 5. The D-state observer firstly determines the rotor flux estimate, and secondly determines the rotor phase estimate from the flux estimate. The D-state observer is constructed according to (12) with an observer gain of $g_1 = 1$ and the replacement of actual speed ω_{2n} by its estimate.

For a salient-pole PMSM, the flux ϕ_i used in the D-state observer in Fig. 6 is determined by means of the average of phase estimate $\hat{\theta}_\gamma$ in phase-locked state as follows:

$$\phi_i \approx [L_i \boldsymbol{I} + L_m \boldsymbol{Q}(0)]\, \boldsymbol{i}_1 = \begin{bmatrix} L_d & 0 \\ 0 & L_q \end{bmatrix} \boldsymbol{i}_1. \quad (29.a)$$

For a nonsalient-pole PMSM, the flux ϕ_i is determined with no necessity of phase estimate as follows:

$$\boldsymbol{\phi}_i = L_i \boldsymbol{i}_1. \quad (29.b)$$

It is worth noting that whatever the rotor speed estimate is, the gain of the feedback loop in the D-state observer is always nonpositive such as $-|\hat{\omega}_{2n}|g_2$ (refer to Fig. 6), and the observer always operates stably.

The phase estimate is determined by means of the rotor flux estimate, such as

$$\left.\begin{aligned} \hat{\boldsymbol{\phi}}_m &= \begin{bmatrix} \hat{\boldsymbol{\phi}}_{md} \\ \hat{\boldsymbol{\phi}}_{mq} \end{bmatrix} \\ \hat{\theta}_\gamma &= \tan^{-1}\frac{\hat{\phi}_{mq}}{\hat{\phi}_{md}} \approx \frac{\hat{\phi}_{mq}}{\Phi} \end{aligned}\right\}. \quad (30)$$

The phase synchronizer is realized exactly based on the generalized integral-type PLL in (24)–(27) or in Fig. 3, and produces estimates of rotor phase evaluated on the α axis, electrical speed, and rotating coordinates speed (refer to Fig. 1).

IV. Experiments

A. Experimental Setup

In order to examine the basic performance of the proposed sensorless vector control method using the D-state observer, extensive experiments were carried out using the equipment illustrated in Fig. 7. The test motor is a 400-W salient-pole PMSM (IPMSM, SST4-20P4AEA-L) made by Yaskawa Electric Corporation (refer to Table I for characteristics). A rotor-mounted encoder is simply for monitoring of the actual rotor N-pole phase and speed, and is not used for control. The load machine is a 3.7-kW dc motor (DK2114V-A02A-D01) of moment of inertia J $= 0.085$ kg $\cdot$ m^2 and rated speed 183 rad/s made by Toyo Denki Seizo K.K. The torque sensor system (TP-5KMCB, DPM-713B) is made by Kyowa Electric Instruments Company Ltd.

Note that the load machine has a 53 times larger moment of inertia than the test motor. This kind of load machine is also useful for examination of the large-inertia accommodation ability of the test motor. Also, note that a minimum number of current and voltage sensors are used in the experiments, i.e. , only two ac current sensors operating from zero frequency and a single dc-link voltage sensor are utilized to realize the proposed sensorless vector control method (refer to Fig. 4).

B. Design of Main Parameters

A single 2×2 observer gain $\boldsymbol{G}$ for the D-state observer was designed according to (14), (19), and (23). More specifically, it was determined simply as $g_1 = g_2 = 1$.

The phase controller for the generalized integral-type PLL was designed as a first-order one in consideration of a huge

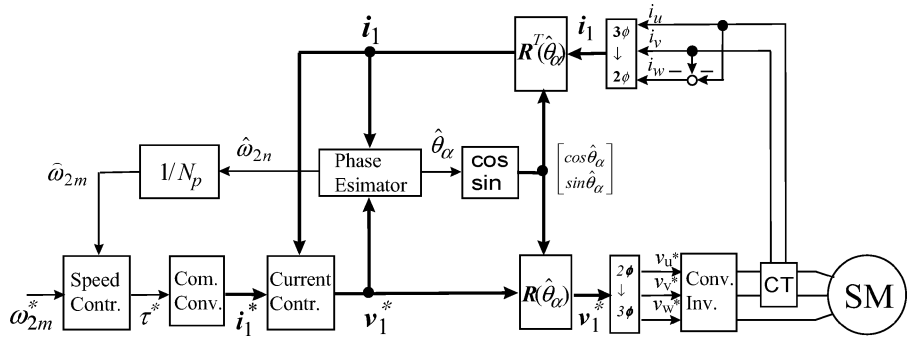

Fig. 4. A configuration of the proposed sensorless vector control system.

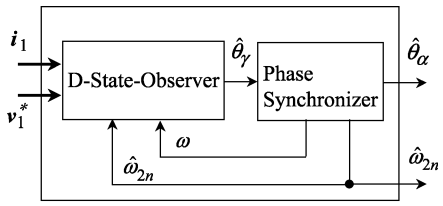

Fig. 5. A configuration of the phase estimator.

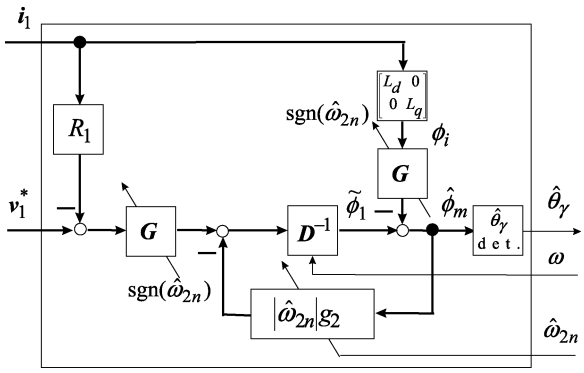

Fig. 6. A configuration of the D-state observer.

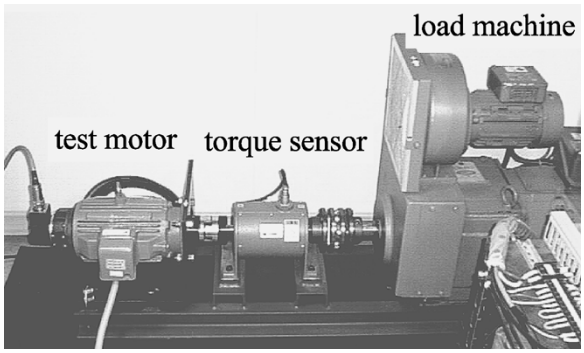

Fig. 7. View of experimental system.

moment of inertia ratio of the load machine coupled with the test motor, i.e.,

$$C_{\mathrm{PLL}}(s) = \frac{c_{n1}s + c_{n0}}{s}. \tag{31}$$

The parameters in (31) are designed such that the Hurwitz polynomial defined in (26) can have two stable zeros at $s = -75$, i.e., $c_{n1} = 150$, $c_{n0} = 5625$.

TABLE I
CHARACTERISTICS OF TEST MOTOR (SST4-20P4AEA-L)

R_1	2.259 (Ω)	rated torque	about 2.2(Nm)
L_i	0.02662(H)	rated speed	183(rad/s)
L_m	- 0.00588(H)	rated current	1.7(A, rms)
Φ	0.2165 (V s/rad)	rated voltage	163(V, rms)
N_p	3	moment of inertia	0.0016(kgm^2)
rated power	400(W)	effective resolution of encoder	4 x 1024(p/r)

The stator current feedback loop was designed so that its bandwidth is 2000 rad/s in consideration of a control period of 125 μs. The current command $\boldsymbol{i}_1^*$ for the feedback loop was converted from torque command τ^* according to the following rule, for simplicity:

$$\boldsymbol{i}_1^* = \begin{bmatrix} 0 \\ \frac{1}{N_p \Phi} \tau^* \end{bmatrix}. \tag{32}$$

The bandwidth of the speed control loop using a proportional–integral (PI) controller was designed to be 2 rad/s in consideration of a huge moment of inertia ratio of the load machine coupled with the test motor. All algorithmic functions from the 3/2 to 2/3 phase converter in Fig. 4 were realized by software on a single digital signal processor (DSP) (floating-point arithmetic TMS320C32-50 MHz from Texas Instruments).

C. Experimental Results of Torque Control

The speed controller was removed from the vector control system in Fig. 4 so that the torque command can be directly injected into the system. Experiments of torque control were carried out in such a way that, firstly, the rotor speed of the test motor was controlled to be a specific one by the load machine, and then, the torque command was injected into the control system for the test motor.

Figs. 8 and 9 show results in motoring and regenerating modes, respectively. They are arranged so that linearity characteristics can be easily evaluated. Each line is associated, from top to bottom, with responses at speeds of 3, 9, 18, 36,

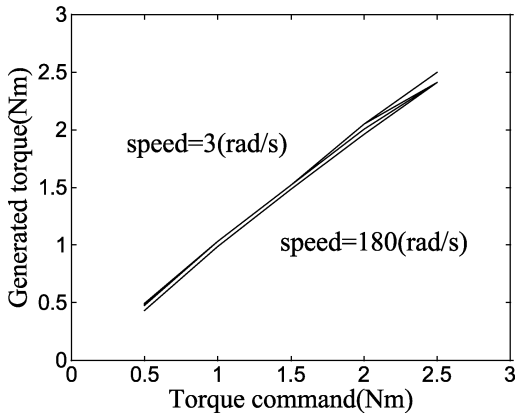

Fig. 8. Torque responses in motoring mode.

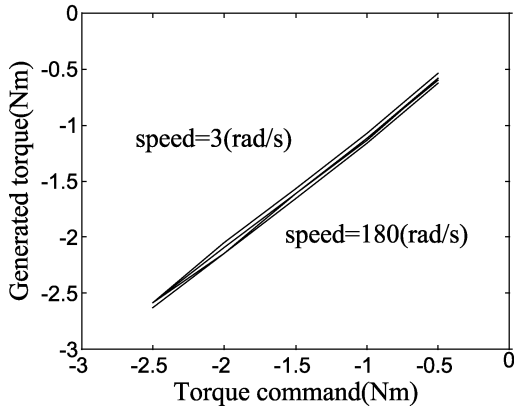

Fig. 9. Torque responses in regenerating mode.

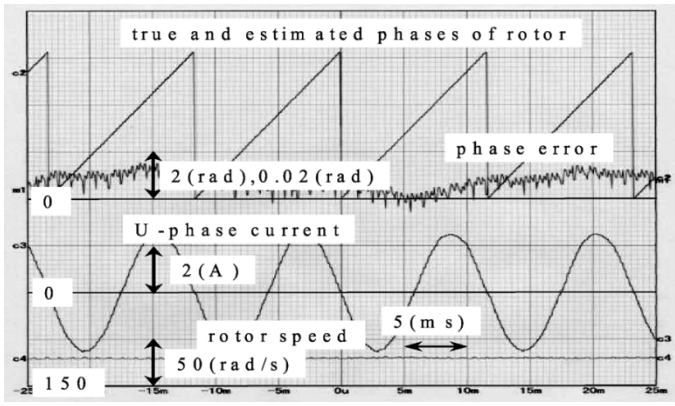

Fig. 10. Steady-state speed response to the rated command of 180 rad/s under rated motoring load.

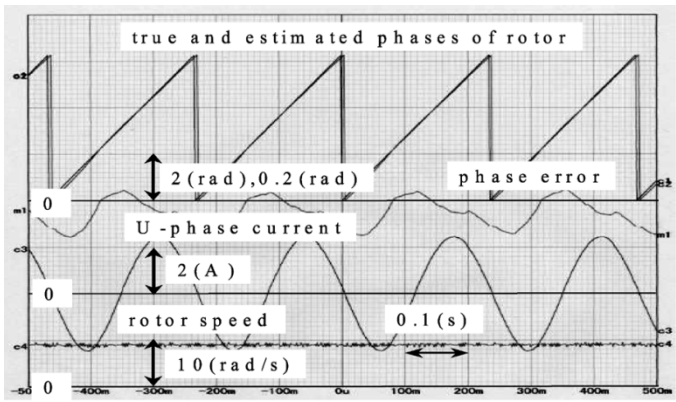

Fig. 11. Steady-state speed response to command of 9 rad/s under rated motoring load.

and 180 rad/s, respectively. Note that the rated speed is about 180 rad/s.

As can be clearly observed, in both modes of motoring and regenerating, good linearity is attained at each constant speed. However, the responses in both modes show slight speed dependency. In motoring mode, generated torque decreases as speed increases. On the other hand, in regenerating mode, generated torque increases as speed increases.

The opposite phenomena result mainly from the same cause, the computing time of 125 μs required for generating the voltage command. Although the phase difference between stator current and rotor is designed to be $\pi/2$ rad as in (32), the actual phase difference decreases in motoring mode, and increases in regenerating mode due to computing time as speed increases. Variation of the phase difference gives rise to that of generating torque. It should be noted that the speed-dependent torque characteristics caused by the computing time appears even for standard sensor vector control as well.

D. Experiment Results of Speed Control

Experiments of speed control were carried out in the system configuration shown in Fig. 4 from several viewpoints of motoring/regenerating, constant/variable speed, instant injection/elimination of load, and zero-speed crossing. The injected load torque was basically set to be rating 2.2 N·m. The current-limiting value was set to be 150% rating in order to resist instant injection of the rated load torque.

1) Steady Response in Motoring Mode:

a) Response at speed of 180 rad/s: Fig. 10 shows a steady-state response of speed control at the rated speed under the rated motoring load. Wavelike data indicate, from the top, actual rotor phase, its estimate, phase estimation error to actual phase, U-phase current, and rotor speed. The time scale is 5 ms/div. The actual rotor phase is directly measured by an encoder of effective 4096 p/r mounted on the rotor of the test motor. It is observed from the wavelike data that the average phase estimation error is about 0.01 rad, and that the phase estimate is in good agreement with the actual one. Consequently, good current and speed responses are attained.

b) Response at speed of 9 (rad/s): Fig. 11 shows a steady-state response at 9 rad/s corresponding to 1/20 rated speed. The meaning of the wavelike data is the same as in Fig. 10. The time scale is 0.1 s/div. The rotor phase estimate very slightly fluctuates around the actual one. The average phase estimation error is about -0.1 rad.

c) Response at speed of 3 rad/s: Fig. 12 shows a steady-state response at 3 rad/s corresponding to 1/60 rated speed. The meaning of the wavelike data is the same as in Fig. 10. The time scale is 0.2 s/div. The rotor phase estimate fluctuates around actual one. Average phase estimation error is about

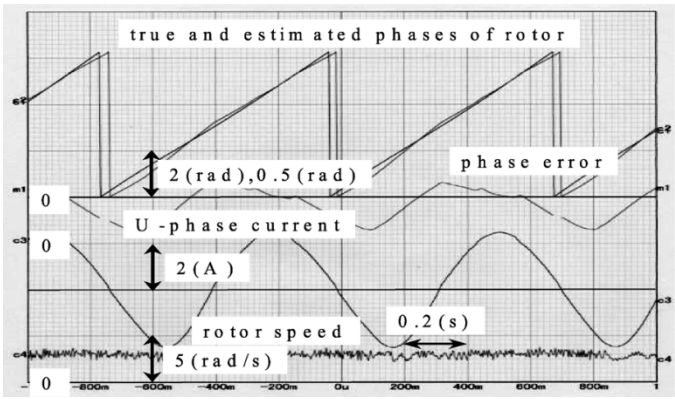

Fig. 12. Steady-state speed response to command of 3 rad/s under rated motoring load.

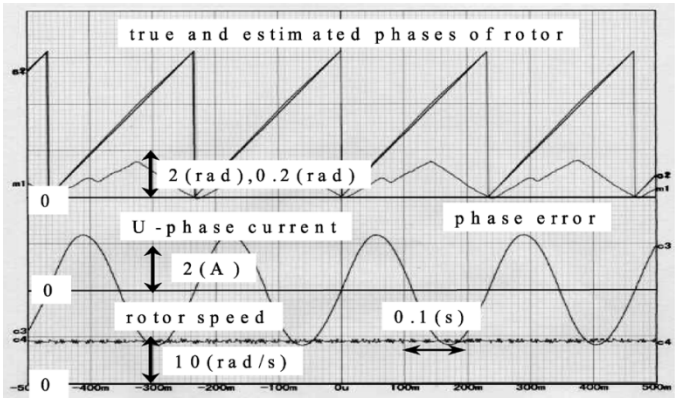

Fig. 13. Steady-state speed response to command of 9 rad/s under rated regenerating load.

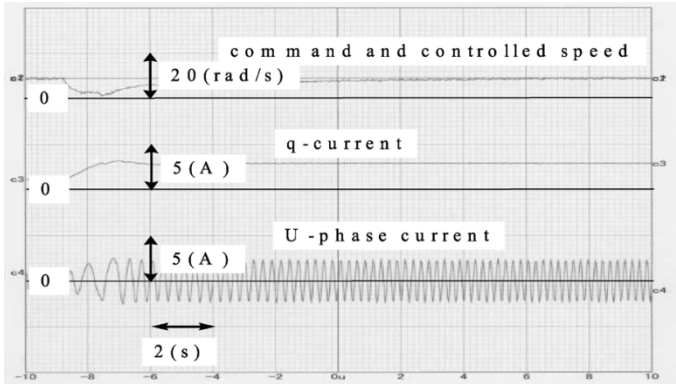

Fig. 14. Transient speed response to instant injection of rated load at speed of 9 rad/s.

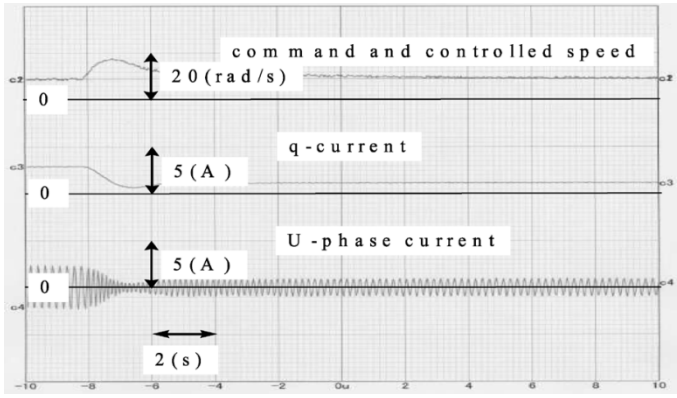

Fig. 15. Transient speed response to instant removal of rated load at speed of 9 rad/s.

-0.2 rad . The fluctuation causes small current distortion and speed variation. As indicated in (23), the error correction rate of the estimate to actual rotor phase by the D-state observer is designed roughly as $\exp(-|\hat{\omega}_{2n}|g_2 t)$. The correction rate in this case turns out to be about $\exp(-9t)$ since the number of pole pairs is three. The slow fluctuation of the estimate is due to the correction rate, which is essentially dominated by rotor speed.

2) Steady Response in Regenerating Mode: Steady-state responses in regenerating mode were similar to those in motoring mode, and no particular difference on which to comment was observed. Fig. 13 illustrates the response at a speed of 9 rad/s for information. As observed, it shows a similar response to that in Fig. 11 except for the sign of the phase estimation error and the phase shift of stator current.

3) Instant Injection and Elimination of Load: One of the most interesting performance features of speed control by sensorless vector control is accommodation of an instantly injected disturbance load. Fig. 14 shows a transient response where rotor speed firstly is controlled at 9 rad/s corresponding to 1/20 rated speed by the proposed vector control system, and then the rated torque load is instantly injected by the load machine. Wavelike data indicate, from top, speed command, its response, q current, and U-phase current, where the time scale is 2 s/div. It is apparent from Fig. 14 that the sensorless vector control system maintains stable operation and removes the influence of the rated disturbance. Note that the large setting time is due to the fact that: 1) the speed bandwidth was designed to be narrow such as 2 rad/s in consideration of a 53 times larger moment of inertia of the load machine and 2) there exists a relatively large friction of the load machine to the test motor.

Fig. 15 shows a transient response where rotor speed firstly is controlled at 9 rad/s under the rated torque load by the proposed vector control system, and the torque load is instantly eliminated. The meaning of the wavelike data is the same as in Fig. 14. The sensorless vector control system operates properly, similarly to that in Fig. 14. The current under no load is for resisting the friction of the load machine.

Similar responses were observed in the speed range from 1/1 to 1/20 rated speed.

4) Slow Zero-Speed Crossing Under Load: As the error equation in (18) implies, the error correction function to the actual phase decreases as rotor speed decreases, and comes to a halt at zero speed. In other words, this suggests that if phase error is small before zero speed, and operating time at zero speed is short, it would be possible to estimate rotor phase continuously, even in the speed range including zero.

Fig. 16 shows the response of the experiment for examining the inference, where the speed command is a trapezoid of amplitude ± 20 rad/s, acceleration ± 30rad/s^2, and load torque including friction is tuned to be the motoring rating at a speed of

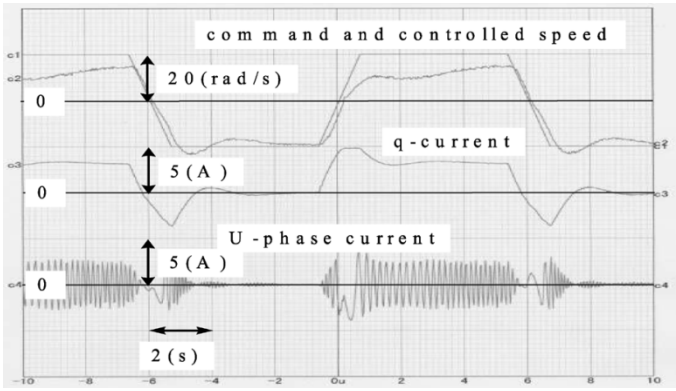

Fig. 16. Slow zero-speed crossing response under load.

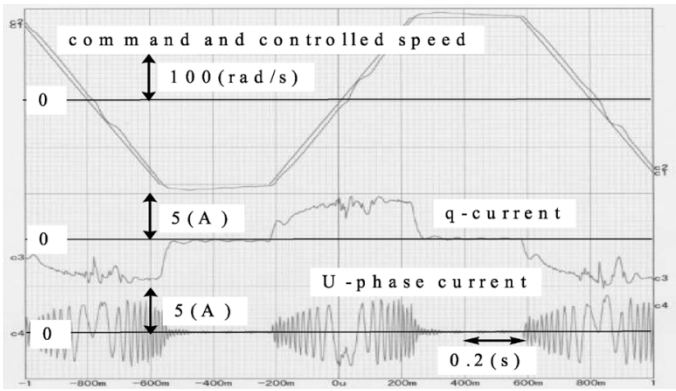

Fig. 17. Speed response to command with zero crossing and acceleration of ± 800 rad/s.

$+20$ rad/s. The wavelike data show, from the top, speed command, its response, q current, and U-phase current. The time scale is 2 s/div. Fig. 16 corroborates the validity of the inference.

At the speed of -20 rad/s, q current goes to almost zero. This means that the tuned load torque is nearly equal to the friction torque by sheer coincidence. Both of them in the experiment will be about 1/2 the rating of the test motor, i.e., about 1.1 N·m.

5) Tracking to Variable-Speed Command With High Acceleration: In order to evaluate the tracking capabilities to the variable-speed command with high acceleration, the load machine was isolated from the test motor, and a coupling of inertia $0.000\,55$ kg $\cdot$ m^2 was attached to the test motor. Consequently, the power rate of the test motor with the coupling results in about 2250 W/s (refer to Table I). In consideration of the power rate and the rated torque, a trapezoid speed command of acceleration ± 800 rad/s^2, amplitude ± 180 rad/s, and period 1.6 s was prepared. The speed bandwidth was redesigned as 50 rad/s with consideration given to the total moment of inertia.

Fig. 17 is the experimental results, which shows, from the top, speed command, its response, q current, and U-phase current. The time scale is 0.2 s/div. Although a small fluctuation appears right after the zero-speed crossing, good tracking capability is attained as a whole. The small fluctuation would be a kind of transient response due to effective restart of the phase error correction function by the D-state observer.

V. Conclusion

This paper has proposed a new D-state-observer-based vector control method, which can be applied to both salient-pole and nonsalient-pole PMSMs. The newly proposed D-state observer has the following attractive features; 1) it requires no additional steady-state condition for the motor mathematical model; 2) its order is the minimum second; 3) a single observer gain is a simple constant over a wide operating range, and it is easily designed; 4) it utilizes motor parameters in a very simple manner; and 5) its structure is very simple and it can be realized at very low computational load. Usefulness of the proposed sensorless vector control method was examined and confirmed through extensive experiments.

The D-state-observer-based vector control method is supposed to be used for the low-to-high-speed region in the manner of the frequency-hybrid combination, where another sensorless method producing continuously appropriate torque in the zero-to-low-speed region and playing a role of starting motors will be employed. There exists at least a sensorless method called "mirror-phase vector control" that can produce 250% rated torque at very low speed including standstill [9]. The D-state-observer-based vector control method has being employed in a low-to-high-speed drive of several industrial devices including a vehicle air-conditioning compressor using carbon dioxide, a sensorless-vector-controlled/transmissionless electric vehicle (EV), etc. [10]. For the EV, the D-state-observer-based vector control and the mirror-phase vector control are used in the manner of the frequency-hybrid combination [9], [10].

References

[1] L. A. Jones and J. H. Lang, "A state observer for the permanent-magnet synchronous motor," *IEEE Trans. Ind. Electron.*, vol. 36, no. 4, pp. 346–354, Aug. 1989.

[2] R. B. Sepe and J. H. Lang, "Real-time observer-based (adaptive) control of a permanent-magnet synchronous motor without mechanical sensors," *IEEE Trans. Ind. Appl.*, vol. 28, no. 6, pp. 1345–1352, Nov./Dec. 1992.

[3] K. Tatematsu, D. Hamada, K. Uchida, S. Wakao, and T. Onuki, "Sensorless control for permanent magnet synchronous motor with reduced order observer," in *Proc. IEEE PESC'98*, Jun. 1998, pp. 125–131.

[4] G. Yang, R. Tomioka, M. Nakano, and T. H. Chin, "Position and speed sensorless control of brushless DC motor based on an adaptive observer," *IEEJ Trans. Ind. Appl.*, vol. 113, pp. 579–586, May 1993.

[5] Y. Kinpara, "Position sensorless control of PM motor using adaptive observer on rotational coordinates," *IEEJ Trans. Ind. Appl.*, vol. 123, pp. 600–609, May 2003.

[6] Y. Yamamoto, Y. Yoshida, and T. Ashikaga, "Sensorless control of PM motor using full order flux observer," *IEEJ Trans. Ind. Appl.*, vol. 124, pp. 743–749, Aug. 2004.

[7] Z. Chen, M. Tomita, S. Doki, and S. Okuma, "The pole assignment of adaptive sliding observers for BLM's sensorless control," in *Nat. Conv. Rec. IEEJ*, vol. 4, Mar. 1998, pp. 286–287.

[8] S. Shinnaka, "A new characteristics-variable two-input/output filter in D-module—Designs, realizations, and equivalence," *IEEE Trans. Ind. Appl.*, vol. 38, no. 5, pp. 1290–1296, Sep./Oct. 2002.

[9] ——, "New mirror-phase vector control for sensorless drive of permanent-magnet synchronous motor with pole saliency," *IEEE Trans. Ind. Appl.*, vol. 40, no. 2, pp. 599–606, Mar./Apr. 2004.

[10] S. Shinnaka and S. Takeuchi, "Development of sensorless vector controlled and transmissionless EV using a high efficient permanent magnet synchronous motor," in *Proc. SICE 4th Annu. Conf. Control Systems*, May 2004, pp. 571–574.

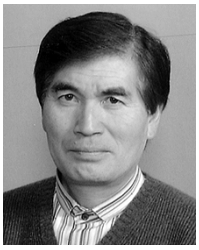

Shinji Shinnaka (M'77) graduated from the National Defense Academy, Yokosuka, Japan, in 1973, received the M.S. and Ph.D. degrees from the University of California, Irvine, in 1977 and 1979, respectively, and received the Dr.Eng. degree from Tokyo Institute of Technology, Tokyo, Japan, in 1990.

After serving with the First Research Institute, Japan Defense Agency, and the Department of Electrical Engineering, National Defense Academy, he was with Canon Inc., as the Head of several research laboratories, from 1986 to 1991. He established a venture research company in the Tokyo area in 1991 and acted as its President. Since 1996, he has been a Professor in the Department of Electrical Engineering, Kanagawa University, Yokohama, Japan. He has worked in a wide range of fields, including communication, information, control engineering, and power electronics, as a researcher, engineer, educator, and director. He developed the first sensorless vector-controlled electrical vehicles with no variable transmission, one of which uses an induction motor, and the other uses a permanent-magnet synchronous motor.

Prof. Shinnaka has received Best Paper, Best Book, and Best Technology Awards from the Society of Instrument and Control Engineers, Japan, and a Prize Paper Award from the IEEE TRANSACTIONS ON INDUSTRY APPLICATIONS.